Proceedings of the 3rd International Conference on Fluid Flow, Heat and Mass Transfer (FFHMT'16)
Ottawa, Canada – May 2 – 3, 2016
Paper No. 145

Natural Convection Simulations of Bingham Fluid within a Square Cavity with Differentially Heated Vertical Walls

Oussama Seghier[1], Lakhdar Rahmani[1], Belkacem Draoui[1], Marc Médale[2], Chérifa Abid[2]
[1]Arid zones energetic laboratory – (ENERGARID), Faculty of Technology / Tahri Mohamed University
BP 417 (08000), Bechar, Algeria
s.osama@hotmail.fr; rahmani_l1@yahoo.fr; bdraoui@yahoo.com
[2]École Polytechnique Universitaire de Marseille, Département de Mécanique Énergétique
Laboratoire IUSTI, UMR 6595 CNRS / Université de Provence Technopôle de Château-Gombert
5 rue Enrico Fermi 13453 Marseille Cedex 13, France
medale@univ-amu.fr; cherifa.abid@univ-amu.fr

Abstract **-** This study presents a numerical simulation of fluid flow and heat transfer due to natural convection within a square chamber (Square Cavity), fully filled with a yield stress fluid obeying the Bingham model of behavior. Two dimensional, steady state, laminar flow with differentially heated vertical walls (Side walls) and insulated horizontal walls (Top and Bottom) have been considered. Plasticity effects on heat mass transfer are investigated for nominal values of Rayleigh number (Ra) in the range of (10^3 to 10^6). We have fixed the Prandtl number (Pr = 10) and Bingham number (Bn = 0.5) to mimic a real incompressible plastic fluid. It is found that the average Nusselt number (Nu*) increases with the increasing of Rayleigh number for the both cases Newtonian and non-Newtonian fluids. However, for the same value of Rayleigh number, the average Nusselt number of Bingham fluid presents a diminution comparing with the Newtonian fluid, due to yield stress effects on the convective term.

Keywords: Natural convection, Numerical simulation, Laminar flow, Square cavity, Bingham fluid, Heat and mass transfer, Nusselt number.

1. Introduction

Natural or free convection, i.e. Buoyancy-driven flow caused by temperature [1], occurs frequently in nature and technological devices. Even the simplicity of the natural case in square and rectangular cavities have numerous engineering applications such as nuclear reactor insulation, room ventilation, solar energy collectors, cooling electronic equipment and energy storage. As a consequence of these applications and its geometrical simplicity, a large number of the existing literature [2-3-4] is available for such flows especially in the case of Newtonian fluid. One of the most studied cases involves two-dimensional square enclosures where the opposing side walls are held isothermally at different temperatures while the other walls (Top and Bottom) are insulated to ensure adiabatic condition, we cite for example the work of Turan et al. [5-6] who studied free convection in a square enclosure filled with yield stress fluids. Although various shaped heated objects configurations totally immersed within the yield stress fluid problems are possible, such as sphere [7], circular and elliptical cylinders [8-9], square cylinder [10-11], semi-circular cylinder [12-13] in unconfined power-law and confined [14] power-law media.

In particular, the coupled-momentum and energy equations have been solved numerically for laminar natural convection from differentially heated vertical walls within a square enclosure completely filled with a Bingham plastic fluid, over the followings ranges of conditions: Rayleigh number ($10^3 \leq Ra \leq 10^6$), Prandtl number (Pr=10), Bingham number (Bn=0.5).

The paper is concluded by presenting comparisons of velocity components (U and V) on the mid-plane, stream function, isothermal layers, Max Nusselt number (Nu_{max}) and average Nusselt number (Nu*) of the both cases, Newtonian fluid (Bn=0) and Non-Newtonian fluid (Bn=0.5) for different nominal values of Rayleigh number.

2. Numerical Method

2.1. Geometry and mesh numbers

Fig.1 presents the schematic diagram of the domain witch the simulation will be run. The mesh numbers have been set on an analysis of three different non-uniform meshes M1 (41x41), M2 (51x51) and M3 (61x61). Based on a reasonable compromise between high accuracy and computational efficiency, M2 was considered efficient for all simulations during this study. Fig. 2 presents the mesh numbers using in this work.

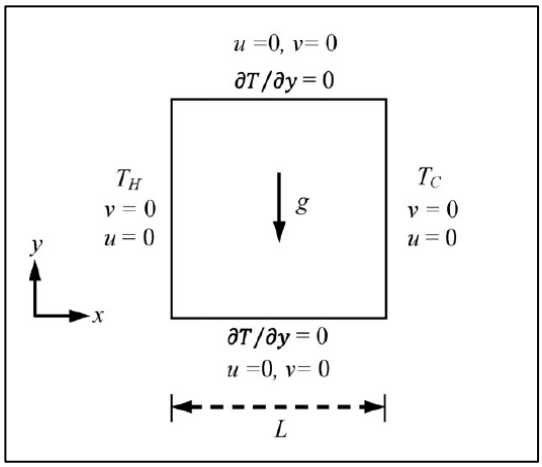

Fig. 1: Layout of the simulation domain.

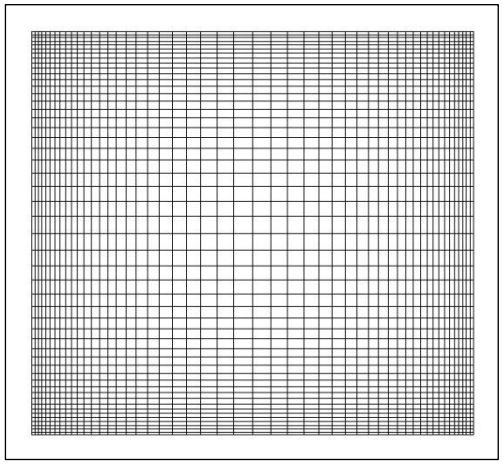
Fig. 2: Non-uniform mesh numbers (51x51).

2.2. Boundary conditions

The two vertical walls of a square enclosure are kept at different temperatures ($T_H > T_C$), whereas the other boundaries are considered to be adiabatic in nature. Both velocity components (i.e. u and v) are identically zero on each boundary because of the no-slip condition and impenetrability of rigid boundaries. The temperatures for cold and hot vertical walls are specified (i.e. T at (x =0) = T_H and T at (x = L) = T_C). The temperature boundary conditions for the horizontal insulated boundaries are given by: $\partial T/\partial y = 0$ at y = 0and y = L. Here 4 governing equations (1 continuity + 2 momentums + 1 energy) for 4 quantities (u, v, p, T) are solved and thus no further boundary conditions are needed for pressure.

2.3. CFD program

Fluent, is the commercial CFD software used to solve the coupled conservation equations of mass, momentum and energy. In the present work, a second-order central differencing scheme is used for diffusive terms and a second-order up-wind scheme for the convective terms. SIMPLE algorithm has been used for coupling of pressure and velocity.

2.4. Mathematical formulation

For incompressible fluids the conservation equations for mass, momentum and energy under steady-state take the following form:

Mass conservation equation:

$$\frac{\partial u_i}{\partial x_i} = 0 \tag{1}$$

Momentum conservation equations:

$$\rho u_j \frac{\partial u_i}{\partial x_j} = -\frac{\partial p}{\partial x_i} + \rho g \delta_{i2} \beta (T - T_c) + \frac{\partial \tau_{ij}}{\partial x_j} \tag{2}$$

Energy conservation equation:

$$\rho u_j Cp \frac{\partial T}{\partial x_j} = \frac{\partial}{\partial x_j}\left(k \frac{\partial T}{\partial x_j}\right) \tag{3}$$

2.5. Validation with the benchmark

The simulation results for Newtonian fluids have also been compared with the well-known benchmark data of de Vahl Davis [2] for Rayleigh numbers Ra ranging from 10^3 to 10^6 and Prandtl number equal to Pr = 0.71. The comparisons between the present simulations results with the corresponding benchmark values are very good and entirely consistent with our grid-dependency studies. The comparison is summarized in Table 1.

Table 1: Comparison of our simulation results with the benchmark of Vahl Davis [2].

		Present results	Benchmark results [2]
$Ra = 10^3$	Nu*	1.118	1.118
	Nu_{max}	1.507	1.505
	U_{max}	3.630	3.649
	V_{max}	3.677	3.697
$Ra = 10^4$	Nu*	2.246	2.243
	Nu_{max}	3.534	3.528
	U_{max}	16.124	16.178
	V_{max}	19.504	19.617
$Ra = 10^5$	Nu*	4.528	4.519
	Nu_{max}	7.756	7.717
	U_{max}	34.686	34.730
	V_{max}	68.140	68.590
$Ra = 10^6$	Nu*	8.875	8.800
	Nu_{max}	17.937	17.925
	U_{max}	64.846	64.630
	V_{max}	217.276	219.360

2.6. Rheological model

A number of empirical models have been proposed for describing the interrelation between shear stress and strain rate in yield stress fluids. The most well-known model, and certainly the oldest, is the Bingham model which, in tensorial form, can be expressed as:

$$\bar{\bar{\dot{\gamma}}} = 0, \quad \text{for} \quad \tau \le \tau_c \tag{4}$$

$$\bar{\bar{\tau}} = \left(\mu + \frac{\tau_c}{\dot{\gamma}}\right)\bar{\bar{\dot{\gamma}}}, \quad \text{for} \quad \tau > \tau_c \tag{5}$$

Where, $\bar{\bar{\dot{\gamma}}}$ the strain tensor, $\bar{\bar{\tau}}$ the stress tensor, τ_c the yield stress, μ the so called plastic viscosity of the yielded fluid. τ And $\dot{\gamma}$ are evaluated based on the second invariants of the stress and shear rate tensors in a pure shear flow, are given by:

$$\tau = \left[\frac{1}{2}\bar{\bar{\tau}} : \bar{\bar{\tau}}\right]^{1/2} \tag{6}$$

$$\dot{\gamma} = \left[\frac{1}{2}\bar{\bar{\dot{\gamma}}} : \bar{\bar{\dot{\gamma}}}\right]^{1/2} \tag{7}$$

The bi-viscosity model [15] has been used to mimic the stress shear-rate characteristics for a Bingham fluid in the following manner:

$$\bar{\bar{\tau}} = \mu_y \bar{\bar{\dot{\gamma}}}, \quad \text{for} \quad \dot{\gamma} \leq \frac{\tau_c}{\mu_y} \tag{8}$$

$$\bar{\bar{\tau}} = \tau_c + \mu \left[\bar{\bar{\dot{\gamma}}} - \frac{\tau_c}{\mu_y}\right], \quad \text{for} \quad \dot{\gamma} > \frac{\tau_c}{\mu_y} \tag{9}$$

2.7. Dimensionless numbers

The Rayleigh number Ra represents the ratio of the strengths of thermal transports due to buoyancy to thermal diffusion, which is defined in the present study in the following manner:

$$\mathrm{Ra} = \frac{\rho^2 \mathrm{Cp}\, g\, \beta\, \Delta T\, L^3}{\mu\, k} = \mathrm{Gr.\,Pr} \tag{10}$$

The Grashof number Gr represents the ratio of the strengths of buoyancy and viscous forces.

$$\mathrm{Gr} = \frac{\rho^2\, g\, \beta\, \Delta T\, L^3}{\mu^2} \tag{11}$$

The Prandtl number Pr depicts the ratio of momentum diffusion to thermal diffusion.

$$\mathrm{Pr} = \frac{\mu\, \mathrm{Cp}}{k} \tag{12}$$

The Nusselt number Nu represents the ratio of heat transfer rate by convection to that by conduction in the fluid in question.

$$\mathrm{Nu} = \frac{h\, L}{k} \tag{13}$$

The Bingham number Bn represents the ratio of yield stress to viscous stresses.

$$\mathrm{Bn} = \frac{\tau_c}{\mu} \sqrt{\frac{L}{g\, \beta\, \Delta T}} \tag{14}$$

3. Results and Discussion

It is important to observe the distributions of velocity components (U and V) respectively Fig. 3 and Fig. 4 and the dimensionless temperature T* Fig. 5 to explain the variation of Nu along the hot-wall Fig. 6, for the both cases Newtonian fluid (A) and Bingham fluid (B).

For lowest Rayleigh number Ra=10^3 the distribution of T* is completely linear and the both vertical and horizontal velocities components are essentially negligible due to very weak flow as the effects of buoyancy forces are dominated by viscous effects. Under this circumstance, the heat transfer takes place entirely by conduction across the enclosure.

With the increasing of Rayleigh number Ra within the enclosure, as a consequence the effects of buoyancy force strengthens relative to the viscous force, which in turn augments heat transfer by convection due to stronger buoyancy-driven flow with higher vertical and horizontal velocity magnitude. This effect is clearly evident from Fig. 3 and Fig. 4, which shows that the both respectively horizontal and vertical velocity magnitude does indeed increase with increasing Ra for the both cases Newtonian and Bingham fluids.

The distribution of non-dimensional temperature becomes increasingly non-linear with the strengthening of convective transport for higher values of Ra for both Newtonian and Bingham fluids Fig. 5.The isotherms layers become

more curved with increasing Rayleigh number due to a strong convective current within the enclosure Fig. 8 and Fig. 10. For the lowest Rayleigh number, contour of static temperature of the case of Bingham fluid are parallel to the side walls due to conduction dominated heat transfer Fig. 10.

The variation of Nusselt number Nu along the hot-wall is shown in Fig. 6. The results show that Nu increases with Ra for both cases Newtonian and Bingham fluids. In addition it can be observed that the values of Nu for Bingham fluids are smaller than that obtained in the case of Newtonian fluids with the same nominal Rayleigh number Ra due to the plasticity effects which are in according with the properties of the non-Newtonian fluid Fig. 7.

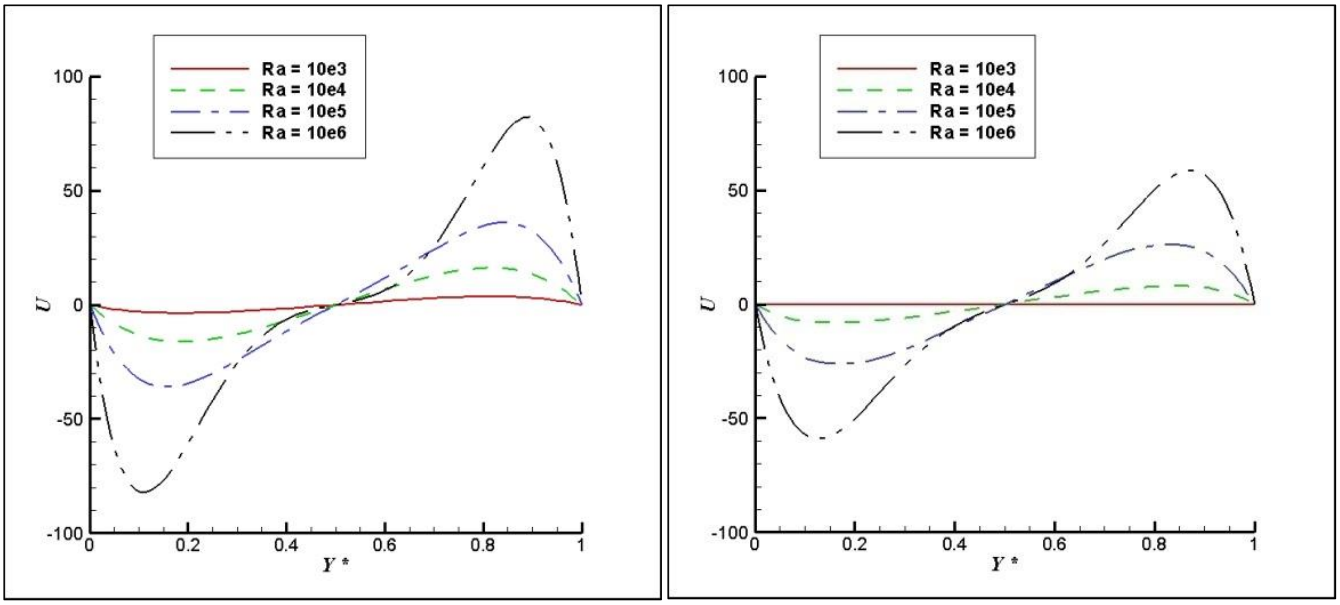

(A) (B)

Fig. 3: Variations of U velocity on the surface x=0.5 for Newtonian fluid (A) and Bingham fluid (B).

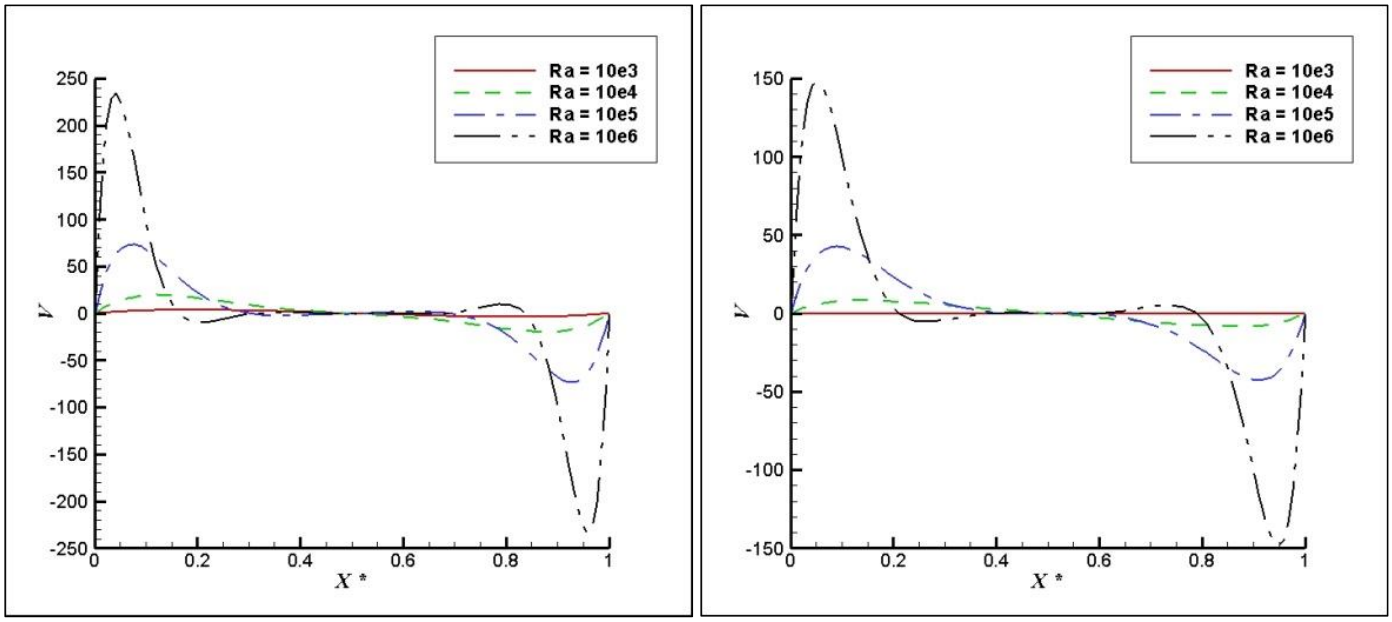

(A) (B)

Fig. 4: Variations of V velocity on the surface y = 0.5 for Newtonian fluid (A) and Bingham fluid (B).

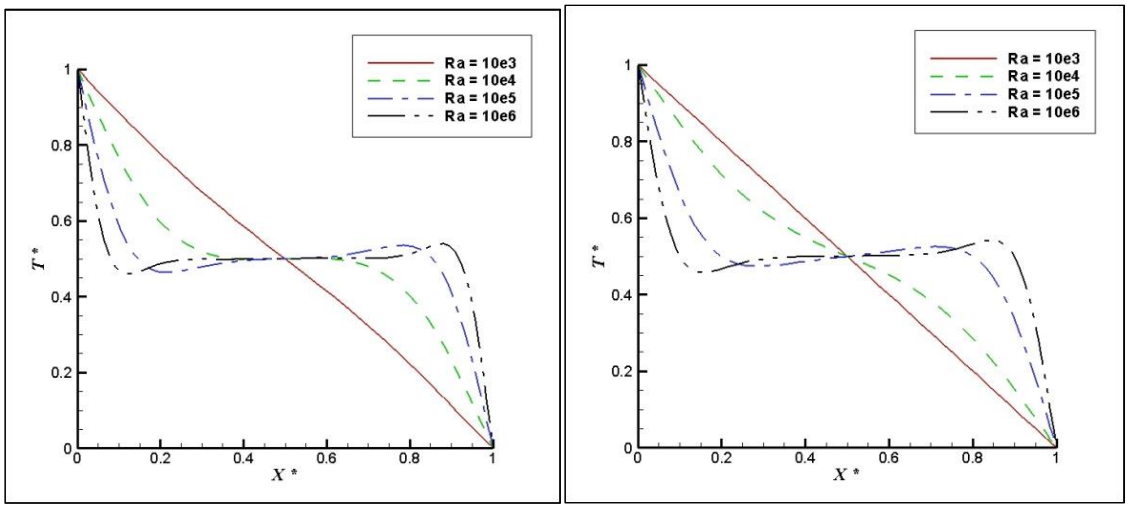

(A) (B)

Fig. 5: Variations of dimensionless temperature T* on the surface y = 0.5 for Newtonian fluid (A) and Bingham fluid (B).

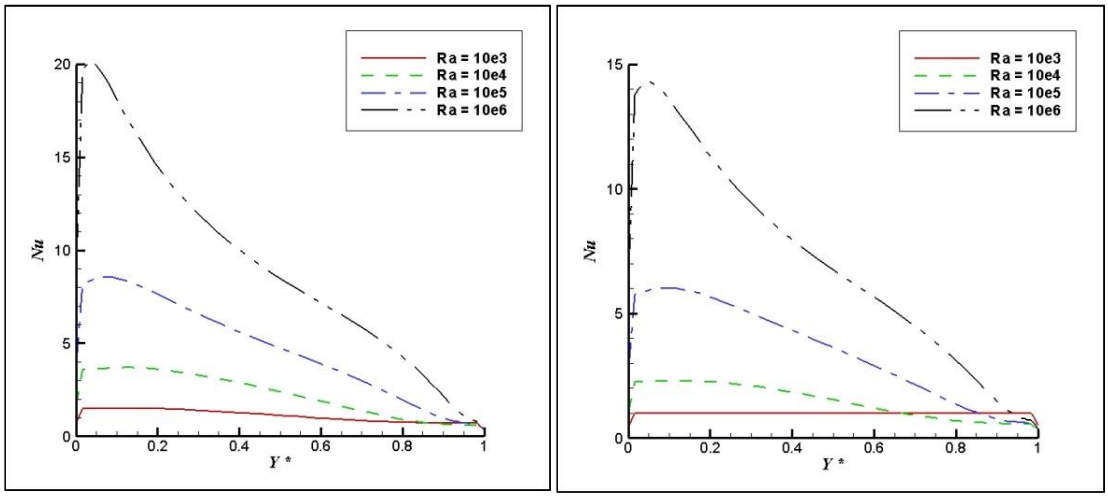

(A) (B)

Fig. 6: Variations of Nusselt number on the hot wall for Newtonian fluid (A) and Bingham fluid (B).

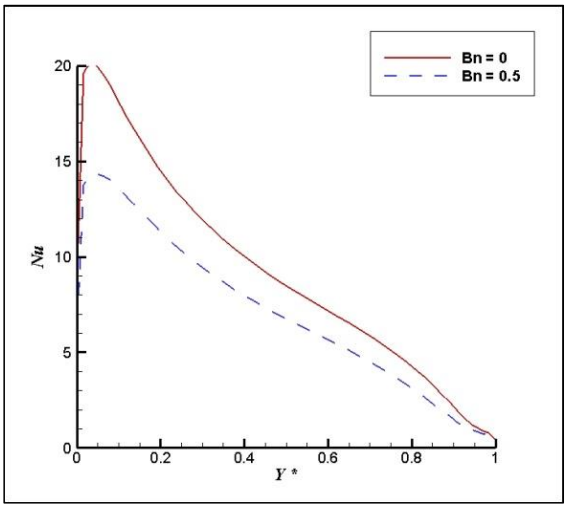

Fig. 7: Comparison of Nusselt number on the hot wall for Newtonian and Bingham fluid for $Ra = 10^6$.

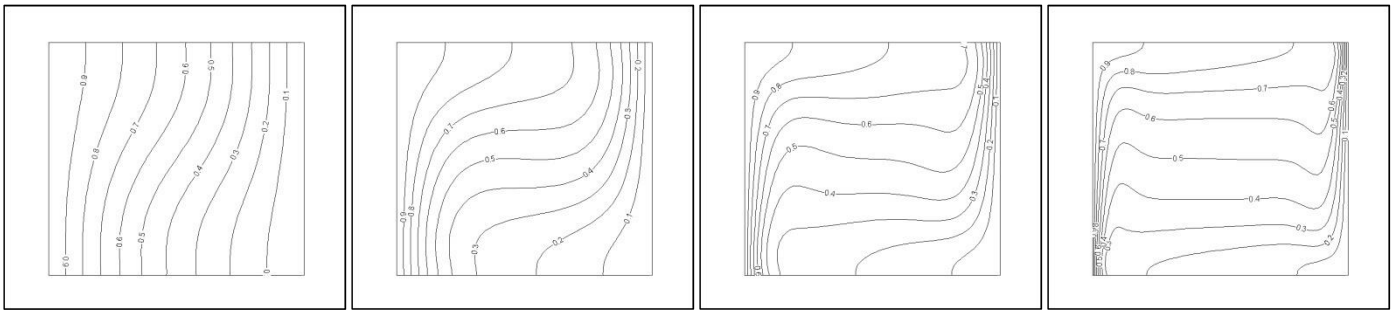

$Ra = 10^3$ $Ra = 10^4$ $Ra = 10^5$ $Ra = 10^6$

Fig. 8: Contours of isotherm layers of Newtonian fluid for different $Ra = 10^3$; 10^4; 10^5 and 10^6.

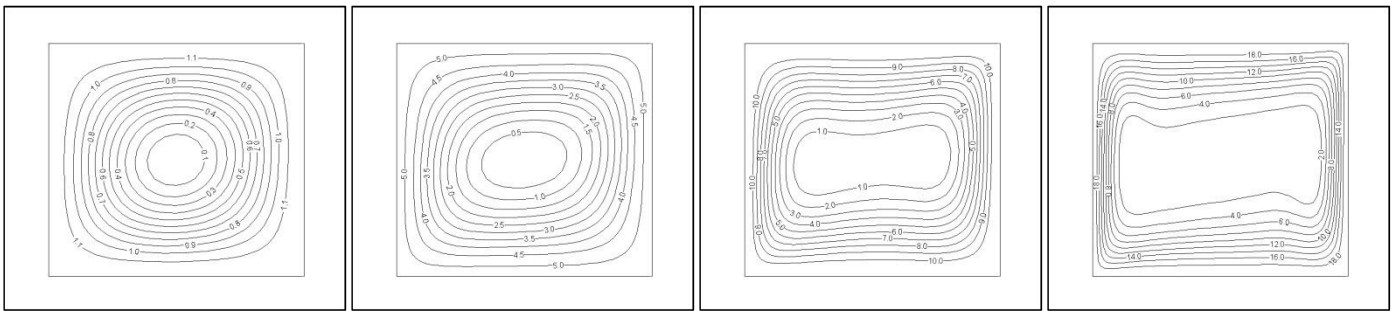

$Ra = 10^3$ $Ra = 10^4$ $Ra = 10^5$ $Ra = 10^6$

Fig. 9: Contours of stream function of Newtonian fluid for different $Ra = 10^3$; 10^4; 10^5 and 10^6.

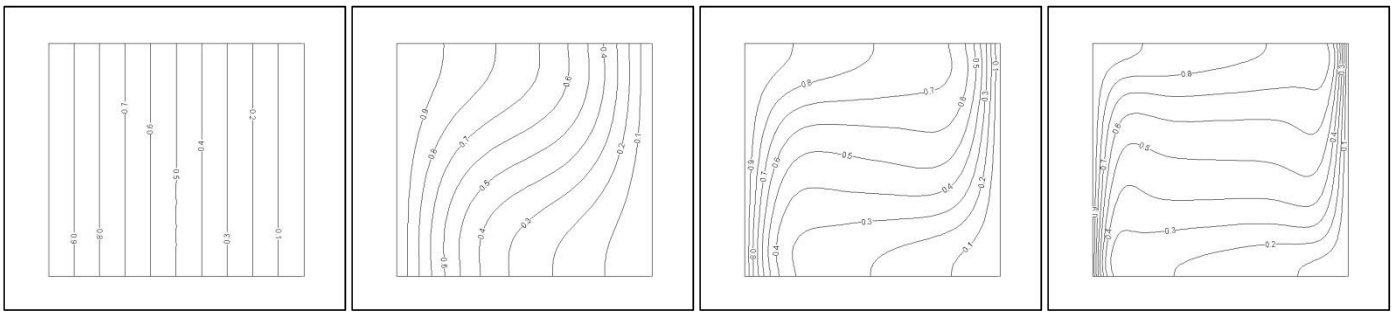

$Ra = 10^3$ $Ra = 10^4$ $Ra = 10^5$ $Ra = 10^6$

Fig. 10: Contours of isotherm layers of Bingham fluid for different $Ra = 10^3$; 10^4; 10^5 and 10^6.

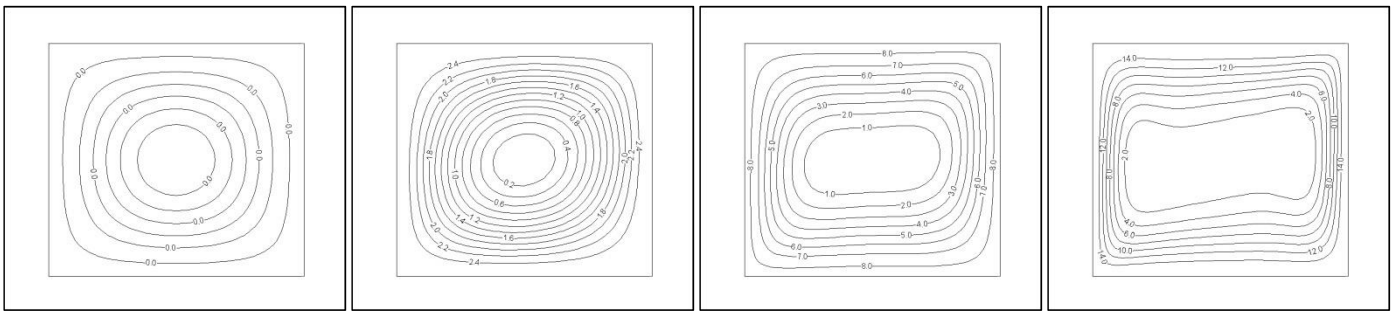

$Ra = 10^3$ $Ra = 10^4$ $Ra = 10^5$ $Ra = 10^6$

Fig. 11: Contours of stream function of Bingham fluid for different $Ra = 10^3$; 10^4; 10^5 and 10^6.

4. Conclusion

This study presents the heat and mass transfer of steady laminar flow due to natural convection of yield stress fluids obeying the Bingham model of behavior in a square cavity with differentially heated vertical walls have been numerically studied.

The effects of Rayleigh number Ra and Bingham number Bn between two cases Newtonian Bn = 0 and Bingham Bn = 0.5 on heat and velocity components (U and V) have been investigated. According to the both profiles of vertical and horizontal velocities, it is found that the mean Nusselt number Nu increases with increasing values of Rayleigh number for both Newtonian and Bingham fluids. However the Nusselt numbers obtained for Bingham fluid which Bn = 0.5 are smaller than those obtained in the case of Newtonian fluid Bn = 0 with the same values of nominal Rayleigh number.

Free convection started in the case of Newtonian fluid at lowest Rayleigh number $Ra = 10^3$, however in the case of Bingham fluid for the same lowest Rayleigh number $Ra = 10^3$ the heat transfer took place principally by conduction, it was clear that the profiles of isotherms are parallel to vertical wall, and the simulation results show that the value of mean Nusselt number settled to unity (i.e. Nu = 1) for $Ra = 10^3$ and Bn = 0.5.

For future numerical studies in the same field of free convection, we think to investigate the effects of geometrical shapes of the enclosure, yield stress (i.e. range of Bn number) and plastic viscosityμ for a deeper understanding of natural convection of yield stress fluids within cavities.

References

[1] S. V. Patankar, *Numerical Heat Transfer and Fluid Flow*. Hemisphere, Washington, DC, 1980.

[2] G. de Vahl Davis, "Natural convection of air in a square cavity: a bench mark numerical solution," *Int. J. Num. Methods Fluids*, vol. 3, pp. 249-264, 1983.

[3] A. F. Emery and J. W. Lee, "The effects of property variations on natural convection in a square cavity," *J. Heat Transfer*, vol. 121, pp. 57-62, 1999.

[4] O. Aydın, A. Unal, and T. Ayhan, "Natural convection in rectangular enclosures heated from one side and cooled from above," *Int. J. Heat Mass Transfer*, vol. 42, pp. 2345-2355, 1999.

[5] O. Turan, N. Chakraborty, and R. J. Poole, "Laminar natural convection of Bingham fluids in a square enclosure with differentially heated side walls," *Journal of Non-Newtonian Fluid Mechanics*, vol. 165, pp. 901-913, 2010.

[6] O. Turan, R. J. Poole, and N. Chakraborty, "Aspect ratio effects in laminar natural convection of Bingham fluids in rectangular enclosures with differentially heated side walls," *Journal of Non-Newtonian Fluid Mechanics*, vol. 166, pp. 208-230, 2011.

[7] A. Prhashanna and R. P. Chhabra, "Free convection in power-law fluids from a heated sphere," *Chemical Engineering Science*, vol. 65, pp. 6190-6205, 2010.

[8] A. Prhashanna and R. P. Chhabra, "Laminar natural convection from a horizontal cylinder in power-law fluids," *Industrial and Engineering Chemistry Research*, vol. 50, pp. 2424-2440, 2011.

[9] C. Sasmal and R. P. Chhabra, "Effect of aspect ratio on natural convection in power law liquids from a heated horizontal elliptic cylinder," *International Journal of Heat and Mass Transfer*, vol. 55, pp. 4886-4899, 2012.

[10] C. Sasmal and R. P. Chhabra, "Laminar natural convection from a heated square cylinder immersed in power-law liquids," *Journal of Non-Newtonian Fluid Mechanics*, vol. 166, pp. 811–830, 2011.

[11] C. Sasmal and R. P. Chhabra, "Effect of orientation on laminar natural convection from a heated square cylinder in power-law fluids," *International Journal of Thermal Sciences*, vol. 57, pp. 112-125, 2012.

[12] A. Chandra and R. P. Chhabra, "Laminar free convection from a horizontal semicircular cylinder to power-law fluids," *International Journal of Heat and Mass Transfer*, vol. 55, pp. 2934-2944, 2012.

[13] A. K. Tiwari and R. P. Chhabra, "Laminar natural convection in power-law liquids from a heated semi-circular cylinder with its flat side oriented downward," *International Journal of Heat and Mass Transfer*, vol. 58, pp. 553-567, 2013.

[14] M. Sairamu and R. P. Chhabra, "Natural convection in power-law fluids from a tilted square in an enclosure," *International Journal of Heat and Mass Transfer*, vol. 56, pp. 319-339, 2013.

[15] E. J. O'Donovan and R. I. Tanner, "Numerical study of the Bingham squeeze film problem," *J. Non-Newtonian Fluid Mech.*, vol. 15, pp. 75-83, 1984.